Solution of a time fractional inverse advection-dispersion problem by discrete mollification

Solución de un problema inverso de advección-dispersión con derivada temporal fraccionaria por medio de molificación discreta

CARLOS MEJÍA[1,✉], ALEJANDRO PIEDRAHITA H.[1,2]

[1]Universidad Nacional de Colombia, Medellín, Colombia

[2]Universidad de Antioquia, Medellín, Colombia

ABSTRACT. We consider an inverse problem for a time fractional advection-dispersion equation in a 1-D semi-infinite setting. The fractional derivative is interpreted in the sense of Caputo and advection and dispersion coefficients are constant. The inverse problem consists on the recovery of the boundary distribution of solute concentration and dispersion flux from measured (noisy) data known at an interior location. This inverse problem is ill-posed and thus the numerical solution must include some regularization technique. Our approach is a finite difference space marching scheme enhanced by adaptive discrete mollification. Error estimates and illustrative numerical examples are provided.

Key words and phrases. Ill-posed problems, Caputo fractional derivative, time fractional inverse advection-dispersion problem, finite differences, mollification.

2010 Mathematics Subject Classification. 35R11, 65M06, 65M32.

RESUMEN. Consideramos un problema inverso para una ecuación de advección-dispersión con derivada temporal fraccionaria, en una configuración unidimensional. La derivada fraccionaria se interpreta en el sentido de Caputo y las coeficientes de advección y de dispersión son constantes. El problema inverso involucra la reconstrucción simultánea de la concentración de soluto y del flujo de dispersión en una de las fronteras del dominio físico, a partir de lecturas de datos perturbados en un punto interior del dominio. Mostramos que

el problema inverso es mal condicionado y por tanto una solución numérica del problema requiere de alguna técnica de regularización. Proponemos un esquema de diferencias finitas de marcha en el espacio, que utiliza molificación discreta como técnica de regularización. Se incluyen estimativos de error y ejemplos numéricos ilustrativos.

Palabras y frases clave. Problemas mal condicionados, derivada fraccionarias de Caputo, problema inverso de advección-dispersión con derivada temporal fraccionaria, diferencias finitas, molificación.

1. Introduction

From a standard advection-dispersion equation, new problems arise by considering fractional time and/or space derivatives. Furthermore, for the new problems it makes sense to consider inverse problems of different types. These mathematical problems have applications in physics, chemistry, biology and several branches of engineering, among others (see [4, 14, 15, 16, 17]). Fractional advection-dispersion equations and the inverse problems based on them are specially valuable in groundwater hydrology and other instances of transport in porous media ([3, 5]).

The main features of the present work are:

(1) An inverse problem based on a time fractional advection-dispersion equation is solved.

(2) The equation is one-dimensional and the evolution takes place in a semi-infinite setting. As a first approximation, this is not a drawback, according to Benson et al. in [3]. They state: *A typical question that a contaminant hydrogeologist wishes to answer is How far and how fast will a tracer move? As a first approximation, this reduces most problems to one spatial dimension.*

(3) The fractional derivative is a Caputo fractional derivative.

(4) The inverse problem is severely ill-posed.

(5) Discrete mollification is the chosen regularization tool.

Several inverse problems based on time fractional differential equations have been successfully solved by discrete mollification ([12, 13]) but to the best of our knowledge, this is the first time that this regularization method is implemented for the stable solution of a time fractional inverse advection-dispersion equation (TFIADP).

The precise statement of the mathematical problem is introduced in the next section. At a first glance, it is similar to the problems in [14] and several papers by Zheng and Wei ([15, 16, 17]). These publications are the main precedents of

this paper and the crucial difference between all of them and our work, is the use of discrete mollification as regularization procedure.

The rest of the paper is organized as follows: As mentioned before, section 2 introduces the mathematical setting. It includes the relevant equations, the ill-posedness of the inverse problem and a short introduction to discrete mollification. Sections 3 and 4 deal with the space marching numerical scheme and they include the proofs of the main results. The numerical examples are in section 5 and the last section is dedicated to some final remarks.

2. Mathematical setting

Whenever an inverse problem is introduced, there is a direct problem in which it is based. In our case is the following:

$$
\begin{aligned}
D_t^{(\alpha)}u + au_x &= du_{xx}, \quad x > 0, \;\; t > 0, \\
u(x,0) &= 0, \quad x > 0, \\
u(0,t) &= \rho(t), \quad t \geq 0, \;\; u(x,t) \;\; \text{bounded as} \;\; x \to \infty,
\end{aligned}
\tag{1}
$$

where u is the solute concentration, u_x is the dispersion flux, the constants $a > 0$, $d > 0$ represent the average fluid velocity and the dispersion coefficient, respectively, and $D_t^{(\alpha)}u$ denotes the Caputo fractional derivative of order α,

$$
D_t^{(\alpha)}u(x,t) := \begin{cases} \dfrac{1}{\Gamma(1-\alpha)} \displaystyle\int_0^t \dfrac{u_t(x,s)}{(t-s)^\alpha}\, ds, & 0 < \alpha < 1, \\[2mm] u_t(x,t), & \alpha = 1. \end{cases}
\tag{2}
$$

We are interested in the following time fractional inverse advection-dispersion problem (TFIADP):

$$
\begin{aligned}
D_t^{(\alpha)}u(x,t) + au_x(x,t) &= du_{xx}(x,t), \quad x > 0, \;\; t > 0, \\
u(1,t) &= \rho(t), \quad t > 0, \;\; \text{data}, \\
u_x(1,t) &= \sigma(t), \quad t > 0, \;\; \text{data}, \\
u(0,t) &= \xi(t), \quad t \geq 0, \;\; \text{unknown}, \\
u_x(0,t) &= \beta(t), \quad t \geq 0, \;\; \text{unknown}, \\
u(x,0) &= 0, \quad x > 0.
\end{aligned}
\tag{3}
$$

The distributed interior data functions ρ and σ are not known exactly. Moreover, their measured approximations ρ^ε and σ^ε satisfy the estimates $\|\rho - \sigma^\varepsilon\|_\infty < \varepsilon$ and $\|\rho - \sigma^\varepsilon\|_\infty < \varepsilon$ for a prescribed maximum level of noise in the data $\varepsilon > 0$.

We are interested in a numerical identification process of ξ and β based on the overdetermined interior data ρ^ε and σ^ε. They are measurements on the

direct problem evolving process. Our scope is the numerical solution of the inverse problem by discrete mollification, and we do not address theoretical issues related to existence, uniqueness and identifiability of the solute concentration u or the flux of solute u_x.

2.1. The discrete mollification operator

The discrete mollification method ([9, 2]) is based on replacing a discrete set of data $y = \{y_j\}_{j \in \mathbb{Z}}$, which may consist of evaluations or cell averages of a real function $y = y(t)$ at equidistant grid points $t_j = t_0 + j\Delta t$, $\Delta t > 0$, $j \in \mathbb{Z}$, by its mollified version $J_\eta y$, where J_η is the *discrete mollification operator* defined by

$$[J_\eta y]_j := \sum_{i=-\eta}^{\eta} w_i y_{j-i}, \quad j \in \mathbb{Z}.$$

Here, the support parameter $\eta \in \mathbb{N}$ indicates the width of the mollification stencil, and the weights w_i satisfy $w_i = w_{-i}$ and $0 \le w_i \le w_{i-1}$ for $i = 1, \ldots, \eta$ along with $\sum_{i=-\eta}^{\eta} w_i = 1$. The weights w_i are defined as follows:

Let $\delta > 0$, $\Delta t > 0$ and $p > 0$. We choose η as the unique non-negative integer such that

$$(\eta - 1/2)\,\Delta t < p\delta \le (\eta + 1/2)\,\Delta t. \tag{4}$$

Actually

$$\eta = \left\lceil \frac{p\delta}{\Delta t} - \frac{1}{2} \right\rceil,$$

where $\lceil \ \rceil$ means the ceiling function. The weights are obtained by numerical integration of the truncated Gaussian kernel

$$\kappa_{p\delta}(t) = \begin{cases} A_p \delta^{-1} \exp(-t^2/\delta^2), & |t| \le p\delta \\ 0, & |t| > p\delta. \end{cases} \tag{5}$$

where the normalization constant

$$A_p = \left(\int_{-p}^{p} \exp(-s^2) ds \right)^{-1}$$

is chosen in such a way that $\int_{\mathbb{R}} \kappa_{p\delta} = 1$. Based on this kernel, the mollification weights are computed by

$$w_i = \int_{t_i}^{t_{i+1}} \kappa_{p\delta}(-s) ds, \tag{6}$$

where

$$t_j = (j - 1/2)\,\Delta t, \ j \in \mathbb{Z}. \tag{7}$$

We usually take $p = 3$ and refer to δ as the mollification parameter, whose role is to determine the shape of the truncated Gaussian kernel.

Chosen in this way, the mollification weights w_j's are independent of Δt, namely,

$$
\begin{aligned}
w_i &= \int_{t_i}^{t_{i+1}} \kappa_{\delta p}(-s)ds = A_p \delta^{-1} \int_{t_i}^{t_{i+1}} \exp\left(-\frac{s^2}{\delta^2}\right) ds \\
&= A_p \int_{t_i/\delta}^{t_{i+1}/\delta} \exp(-s^2)ds.
\end{aligned}
$$

Recall that

$$\frac{t_i}{\delta} = p\frac{(i - 1/2)\,\Delta t}{(\eta + 1/2)\,\Delta t} = p\frac{(i - 1/2)}{(\eta + 1/2)},$$

then the w_i's depend only on p, δ and η. Some weights are shown in Table 1.

η	w_0	w_1	w_2	w_3	w_4	w_5
1	8.4272e-1	7.8640e-2				
2	6.0387e-1	1.9262e-1	5.4438e-3			
3	4.5556e-1	2.3772e-1	3.3291e-2	1.2099e-3		
4	3.6266e-1	2.4003e-1	6.9440e-2	8.7275e-3	4.7268e-4	
5	3.0028e-1	2.2625e-1	9.6723e-2	2.3430e-2	3.2095e-3	2.4798e-4

TABLE 1. Mollification weights

Remark 2.1. Discrete mollification is a convolution operator and as such, it requires η values to the right and to the left of any given point. Suppose the function $g(t)$ is defined in $I = [0, 1]$. Then, unless some extensions to the left of 0 and to the right of 1 are established, the only points at which discrete mollification can be computed are points of the interval $I_\delta = [p\delta, 1 - p\delta]$. Some useful extensions of the data outside the interval are presented in [2]. However, in this paper, our estimates are given for the interior points of the interval I_δ. All mollifications in this paper are with respect to the time variable, due to the fact that a space marching finite difference scheme is implemented.

Discrete mollification satisfies the following estimates (see [7] and [8]).

Theorem 2.2. *Let g be a sufficiently smooth real function bounded in $\mathbb{R}$. Let G be its discrete version defined on T, a uniform meshgrid with discretization parameter Δt. If G^ε is other discrete function defined on T and satisfies*

$$|G^\varepsilon(t_j) - G(t_j)| \leq \varepsilon \quad \text{for } t_j \in T,$$

then there is a constant $C > 0$ independent of δ such that

$$|J_\eta G^\varepsilon(t_j) - J_\eta G(t_j)| \leq \varepsilon,$$
$$|J_\eta G(t_j) - g(t_j)| \leq C(\delta + \Delta t).$$

Also,

$$\| (J_\eta g^\varepsilon)' - (J_\eta g)' \|_{\infty, I_\delta} \leq 2A_p \frac{\varepsilon}{\delta}.$$

2.2. Fractional derivatives and mollification

The presence of a derivative inside the integral in (2) is an indicator of the ill-conditioning of Caputo fractional derivatives when applied to noisy data. More precisely, if $D^{(\alpha)}g$ is sought but we only have an approximation of $g(t)$ denoted by g^ε and satisfying $\|g - g^\varepsilon\|_\infty < \varepsilon$, instead of recovering $D^{(\alpha)}g$ we look for a mollified approximation $J_\eta \left(D^{(\alpha)} g^\varepsilon \right)$. This approximation satisfies the following error estimate ([13]):

Lemma 2.3. *Let $\varepsilon > 0$, g and g^ε defined on I so that $\|g - g^\varepsilon\|_\infty < \varepsilon$. Additionally, suppose $g \in C^1(I_\delta)$ and both g' and g^ε are uniformly Lipschitz on I_δ. Then there exists a constant C, independent of δ, such that*

$$\left\| J_\eta \left(D^{(\alpha)} g^\varepsilon \right) - D^{(\alpha)} g \right\|_{\infty, I_\delta} \leq \frac{C}{(1 - \alpha)\Gamma(1 - \alpha)} \left(\delta + \frac{\varepsilon}{\delta} \right) \qquad (8)$$

Remark 2.4. The right-hand side of (8) includes the factor $\left(\delta + \frac{\varepsilon}{\delta} \right)$ as a clear indication that computing the Caputo fractional derivative of a noisy approximation of the actual function, is an ill-posed problem. To obtain a formal convergence estimate, the parameters ε and δ have to be linked in order for the right-hand side to tend to 0 as ε tends to ∞.

A discrete approximation of the Caputo fractional derivative can be obtained by a quadrature formula as described in [13]:

Lemma 2.5. *Let g be a continuously differentiable function, and let k be a positive integer. Then the operator*

$$\left(C^{(\alpha)} g \right)(t) := \sigma_{\alpha,k} \sum_{i=0}^{\lfloor t/k \rfloor} \omega_i^{(\alpha)} \left\{ g(t - ik + 1) - g(t - ik) \right\}, \qquad (9)$$

where $\lfloor \quad \rfloor$ *denotes the floor function,*

$$\sigma_{\alpha,k} := \frac{1}{\Gamma(1-\alpha)} \frac{1}{1-\alpha} \frac{1}{k^\alpha} \qquad and \qquad \omega_i^{(\alpha)} := i^{1-\alpha} - (i-1)^{1-\alpha}, \qquad (10)$$

satisfies the first order approximation

$$D^{(\alpha)}g(t) = C^{(\alpha)}g(t) + O(k). \qquad (11)$$

2.3. Mollified problem

The inverse problem (3) is a severely ill-posed problem in the high frequency components as the following argument indicates. We assume that all the functions can be extended to the whole line $-\infty < t < \infty$ by defining them to be zero for $t < 0$, and that lie in $L^2(\mathbb{R})$ with respect to the variable t. Applying the Fourier transform with respect to t at $D_t^{(\alpha)}u + au_x = du_{xx}$, $0 < x < 1$, we obtain [6, p. 17] the second-order differential equation

$$(i\omega)^\alpha \, \widehat{u}(x,\omega) + a \, \widehat{u}_x(x,\omega) = d \, \widehat{u}_{xx}(x,\omega), \quad 0 < x < 1, \quad -\infty < \omega < \infty, \quad (12)$$

where $(i\omega)^\alpha = |\omega|^\alpha e^{i\varsigma\pi\alpha/2}$ and $\varsigma := \mathrm{sgn}(\omega)$. The general solution of (12) is given by

$$\widehat{u}(x,\omega) = Ae^{k_1 x} + Be^{k_2 x}, \qquad (13)$$

where k_1 and k_2 are the two square roots of the complex number $a^2 + 4d(i\omega)^\alpha$, *i.e.*,

$$k_1 := \left| a^2 + 4d(i\omega)^\alpha \right|^{1/2} \left(\cos\frac{\theta}{2} + i\sin\frac{\theta}{2} \right) \qquad and \qquad k_2 := -k_1,$$

with

$$\theta = \arg\left(a^2 + 4d(i\omega)^\alpha \right) = \tan^{-1} \left(\frac{4d|\omega|^\alpha \sin\frac{\varsigma\pi\alpha}{2}}{a^2 + 4d|\omega|^\alpha \cos\frac{\varsigma\pi\alpha}{2}} \right). \qquad (14)$$

Setting $\mu := \left| a^2 + 4d(i\omega)^\alpha \right|^{1/2}$ and $\nu := \cos\frac{\theta}{2} + i\sin\frac{\varsigma\theta}{2}$, the general solution (13) and its derivative can be rewritten in the form

$$\widehat{u}(x,\omega) = Ae^{\mu\nu x} + Be^{-\mu\nu x} \qquad and \qquad \widehat{u}_x(x,\omega) = \mu\nu Ae^{\mu\nu x} - \mu\nu Be^{-\mu\nu x}. \quad (15)$$

When $x = 0$, it follows from expressions (15), using data from inverse problem (3), that

$$\widehat{\rho}(\omega) = A + B,$$
$$\widehat{\sigma}(\omega) = \mu\nu A - \mu\nu B.$$

Solving this system for A and B, we get

$$\begin{bmatrix} A \\ B \end{bmatrix} = \frac{1}{2\mu\nu} \begin{bmatrix} \mu\nu & 1 \\ \mu\nu & -1 \end{bmatrix} \begin{bmatrix} \widehat{\rho}(\omega) \\ \widehat{\sigma}(\omega) \end{bmatrix}. \qquad (16)$$

On the other hand, using the unknowns of the inverse problem (3) when $x = 1$, we get

$$\begin{bmatrix} \widehat{\xi}(\omega) \\ \widehat{\beta}(\omega) \end{bmatrix} = \begin{bmatrix} e^{\mu\nu} & e^{-\mu\nu} \\ \mu\nu e^{\mu\nu} & -\mu\nu e^{-\mu\nu} \end{bmatrix} \begin{bmatrix} A \\ B \end{bmatrix} \tag{17}$$

We derive from (16) and (17) that

$$\begin{bmatrix} \widehat{\xi}(\omega) \\ \widehat{\beta}(\omega) \end{bmatrix} = \frac{1}{2\mu\nu} \begin{bmatrix} e^{\mu\nu} & e^{-\mu\nu} \\ \mu\nu e^{\mu\nu} & -\mu\nu e^{-\mu\nu} \end{bmatrix} \begin{bmatrix} \mu\nu & 1 \\ \mu\nu & -1 \end{bmatrix} \begin{bmatrix} \widehat{\rho}(\omega) \\ \widehat{\sigma}(\omega) \end{bmatrix}.$$

Thus,

$$\begin{bmatrix} \widehat{\xi}(\omega) \\ \widehat{\beta}(\omega) \end{bmatrix} = \begin{bmatrix} \cosh\mu\nu & \frac{1}{\mu\nu}\sinh\mu\nu \\ \mu\nu\sinh h\mu\nu & \cosh\mu\nu \end{bmatrix} \begin{bmatrix} \widehat{\rho}(\omega) \\ \widehat{\sigma}(\omega) \end{bmatrix}.$$

Since

$$\left|a^2 + 4d(i\omega)^\alpha\right|^{1/2} = \left(a^4 + 16d^2|\omega|^{2\alpha} + 8da^2|\omega|^\alpha \cos\frac{\alpha\pi}{2}\right)^{1/4} \to \infty$$

and

$$\theta = \tan^{-1}\left(\frac{4d|\omega|^\alpha \sin\frac{\varsigma\pi\alpha}{2}}{a^2 + 4d|\omega|^\alpha \cos\frac{\varsigma\pi\alpha}{2}}\right) \to \frac{\varsigma\pi\alpha}{2}$$

whenever $|\omega| \to \infty$, it follows that

$$|\cosh\mu\nu| = \left|\cosh\left(\left|a^2 + 4d(i\omega)^\alpha\right|^{1/2}\left[\cos\frac{\theta}{2} + i\sin\frac{\varsigma\theta}{2}\right]\right)\right| \to \infty$$

and

$$|\sinh\mu\nu| = \left|\sinh\left(\left|a^2 + 4d(i\omega)^\alpha\right|^{1/2}\left[\cos\frac{\theta}{2} + i\sin\frac{\varsigma\theta}{2}\right]\right)\right| \to \infty$$

whenever $|\omega| \to \infty$ and therefore solving the inverse problem (3), *i.e.*, obtaining ξ and β from ρ and σ, amplifies the error in a high-frequency component by the factor $\exp\left(\left|a^2 + 4d(i\omega)^\alpha\right|^{1/2}\right)$, showing that the TFIADP is highly ill posed in the high-frequency components.

In the stabilized (mollified) problem, $v := J_\delta u$ and $v_x := J_\delta u_x$ satisfy

$$\begin{aligned}
D_t^{(\alpha)}v(x,t) + av_x(x,t) &= dv_{xx}(x,t), & x > 0, \quad t > 0, \\
v(1,t) &= J_\delta\rho^\varepsilon(t), & t > 0, \quad \text{data}, \\
v_x(1,t) &= J_\delta\sigma^\varepsilon(t), & t > 0, \quad \text{data}, \\
v(0,t) &= J_\delta\xi(t), & t \geq 0, \quad \text{unknown}, \\
v_x(0,t) &= J_\delta\beta(t), & t \geq 0, \quad \text{unknown}, \\
v(x,0) &= 0, & x \geq 0,
\end{aligned} \tag{18}$$

where $D_t^{(\alpha)}v = D_t^{(\alpha)}(J_\delta u) = J_\delta\left(D_t^{(\alpha)}u\right)$ as stated in [10].

3. Mollified space marching finite difference scheme

Let τ be a positive real number and let $\Delta x = h$ and $\Delta t = k$ be the parameters of the finite difference discretization. For each $m \in \{0, \ldots, M\}$ with $M := \left\lceil \frac{1}{h} \right\rceil$, and each $n \in \{0, \ldots, N\}$ with $N := \left\lceil \frac{\tau}{k} \right\rceil$, we denote by R_m^n, W_m^n, and Q_m^n the computed approximations of the mollified solute concentration $v(mh, nk)$, mollified flux of solute $v_x(mh, nk)$, and time fractional partial derivative of time partial derivative of mollified solute concentration $D_t^{(\alpha)} v(mh, nk)$, respectively. Following Murio [12], the space marching finite difference scheme proposed is given by the system

$$R_{m-1}^n = R_m^n - hW_m^n,$$

$$W_{m-1}^n := \left(1 - \frac{a}{d}h\right) W_m^n - \frac{h}{d} Q_m^n, \qquad (19)$$

$$m = M, M - 1, \ldots, 1 \quad \text{and} \quad n = 1, \ldots, N.$$

The values of R_0^n and W_0^n, $n = 1, \ldots, N$, are the calculated approximations for the exact solute concentration $\xi(nk)$ and dispersion flux $\beta(nk)$, respectively, at the grid points of the active boundary $x = 0$.

The next algorithm uses the finite differences scheme (19) to approximate the solution of the mollified problem (18). Notice that the evaluation of the time fractional derivative has to be performed in the indicated increasing order of values of time at each space grid position.

Algorithm 1 Mollified space marching algorithm

Require: Parameters α, a, h, and k, and perturbed data ρ^ε and σ^ε.
Ensure: R_0^n and W_0^n, $n = 0, \ldots, N$.
1: Compute $\sigma_{\alpha,k}$ and $\omega_i^{(\alpha)}$, $i = 0, \ldots, N$.
2: $R_m^0 \leftarrow 0$, $m = 0, \ldots, M$.
3: **for** $n = 1$ until N **do**
4:     $R_M^n \leftarrow J_{\delta_1^0} \rho^\varepsilon(nk)$, automatically obtaining δ_1^0, [1].
5:     $W_N^n \leftarrow J_{\delta_2^0} \sigma^\varepsilon(nk)$, automatically obtaining δ_2^0, [1].
6:     $Q_M^n \leftarrow C^{(\alpha)}\left(J_{\delta_1^0} \rho^\varepsilon(nk)\right)$.
7: **end for**
8: **for** $m = M$ until 1 **do**
9:     $R_{m-1}^n \leftarrow R_m^n - hW_m^n$, $n = 1, \ldots, N$.
10:     $Q_m^n \leftarrow C^{(\alpha)}\left(J_{\delta_1^m} R_m^n\right)$, $n = 1, \ldots, N$, automatically obtaining δ_1^m, [1].
11:     $W_{m-1}^n \leftarrow \left(1 - \frac{a}{d}h\right) W_m^n - \frac{h}{d} Q_m^n$, $n = 1, \ldots, N$.
12: **end for**

Remark 3.1. $R_M^n = J_\eta\left(\rho^\varepsilon(nk)\right)$, $W_M^n = J_\eta\left(\sigma^\varepsilon(nk)\right)$, and $Q_M^n = C^{(\alpha)}\left(J_\eta \rho^\varepsilon(nk)\right)$ are obtained from the noisy data.

For error estimates, we introduce the discrete error functions

$$\Delta R_m^n := R_m^n - v(mh, nk), \qquad \Delta W_m^n := W_m^n - v_x(mh, nk), \qquad (20)$$

for each $m \in \{0, \ldots, M\}$, and each $n \in \{0, \ldots, N\}$. We also define

$$|\Delta R_m| := \max_{0 \leq n \leq N} |\Delta R_m^n|, \qquad |\Delta W_m| := \max_{0 \leq n \leq N} |\Delta W_m^n|. \qquad (21)$$

for each $m \in \{0, \ldots, M\}$.

Lemma 3.2. *There exists a constant $E > 0$ such that*

$$\max\{|\Delta R_M|, |\Delta W_M|\} \leq E(\delta + k). \qquad (22)$$

Proof. By Theorem (2.2), for each $n \in \{0, \ldots, N\}$, there exist positive constants C_n y D_n such that

$$|\Delta R_M^n| = |R_M^n - v(M, nk)| = |J_\eta(\rho^\varepsilon(nk)) - v(0, nk)| \leq C_n(\delta + k)$$

and

$$|\Delta W_M^n| = |W_M^n - v_x(M, nk)| = |J_\eta(\sigma^\varepsilon(nk)) - v_x(0, nk)| \leq D_n(\delta + k),$$

and consequently

$$\max\{|\Delta R_M^n|, |\Delta W_M^n|\} \leq E(\delta + k),$$

with $E := \max\{C_n, D_n \mid n = 0, \ldots, N\}$. By taking the maximum over n, the desired result is obtained. ☑

The next lemma shows the effect of the mollification in the discrete approximation of the Caputo fractional derivative.

Lemma 3.3. *There exists a constant $C_\alpha > 0$ such that*

$$\left| Q_m^n - D_t^{(\alpha)} v(mh, nk) \right| \leq C_\alpha \frac{\varepsilon}{\delta} + O(k). \qquad (23)$$

Proof. By lemma 2.5 and theorem 2.2,

$$\begin{aligned}
\left| Q_m^n - D_t^{(\alpha)} v(mh, nk) \right| &= \left| D_t^{(\alpha)} J_\delta u^\varepsilon(mh, nk) - D_t^{(\alpha)} J_\delta u(mh, nk) + O(k) \right| \\
&\leq \frac{1}{\Gamma(1-\alpha)} \int_0^{nk} \frac{C\varepsilon/\delta}{(nk-s)^\alpha} ds + O(k) \\
&\leq \frac{C}{\Gamma(1-\alpha)} \frac{\varepsilon}{\delta} \frac{(nk)^{1-\alpha}}{1-\alpha} + O(k) \\
&\leq C_\alpha \frac{\varepsilon}{\delta} + O(k).
\end{aligned}$$

☑

Theorem 3.4 (formal convergence of the algorithm). *The mollified space marching algorithm* (1) *converges to the solution of the inverse problem* (3).

Proof. Without loss of generality, assume the dispersion coefficient $d = 1$. Expanding the mollified solute concentration $v(x, t)$ by the Taylor series, we obtain

$$v((m-1)h, nk) = v(mh, nk) - hv_x(mh, nk) + O\left(h^2\right),$$

$$v_x((m-1)h, nk) = v_x(mh, nk) - h\left(D_t^{(\alpha)}v(mh, nk) + av_x(mh, nk)\right) + O\left(h^2\right).$$

Hence the discrete errors (20) can be expressed as

$$
\begin{aligned}
\Delta R_{m-1}^n &= R_{m-1}^n - v((m-1)h, nk) \\
&= R_m^n - hW_m^n - v((m-1)h, nk) \\
&= R_m^n - hW_m^n - v(mh, nk) + hv_x(mh, nk) + O\left(h^2\right) \qquad (24)\\
&= (R_m^n - v(mh, nk)) - h\left(W_m^n - v_x(mh, nk)\right) + O\left(h^2\right) \\
&= \Delta R_m^n - h\Delta W_m^n + O\left(h^2\right),
\end{aligned}
$$

and

$$
\begin{aligned}
\Delta W_{m-1}^n &= W_{m-1}^n - v_x((m-1)h, nk) \\
&= (1-ah)W_m^n - hQ_m^n - v_x(mh, nk) \\
&\quad + h\left(D_t^{(\alpha)}v(mh, nk) + av_x(mh, nk)\right) + O\left(h^2\right) \\
&= (1-ah)W_m^n - hQ_m^n - (1-ah)v_x(mh, nk) \\
&\quad + hD_t^{(\alpha)}v(mh, nk) + O\left(h^2\right) \qquad (25)\\
&= (1-ah)\left(W_m^n - v_x(mh, nk)\right) \\
&\quad - h\left[Q_m^n - \left(D_t^{(\alpha)}v(mh, nk)\right)\right] + O\left(h^2\right) \\
&= (1-ah)\Delta W_m^n + hC_\alpha\frac{\varepsilon}{\delta} + O(hk) + O\left(h^2\right).
\end{aligned}
$$

It follows from (24) and (25) that

$$
\begin{aligned}
\left|\Delta R_{m-1}^n\right| &\leq |\Delta R_m^n| + h\,|\Delta W_m^n| + O\left(h^2\right) \\
&\leq \max_{0\leq n\leq N}|\Delta R_m^n| + h\cdot\max_{0\leq n\leq N}|\Delta W_m^n| + O\left(h^2\right) \\
&\leq |\Delta R_m| + h\,|\Delta W_m| + O\left(h^2\right),
\end{aligned}
$$

and

$$
\begin{aligned}
\left|\Delta W_{m-1}^n\right| &\leq |1-ah|\,|\Delta W_m^n| + O(hk) + O\left(h^2\right) \\
&\leq |1-ah|\cdot\max_{0\leq n\leq N}|\Delta W_m^n| + O(hk) + O\left(h^2\right) \\
&= |1-ah|\,|\Delta W_m| + hC_\alpha\frac{\varepsilon}{\delta} + O(hk) + O\left(h^2\right),
\end{aligned}
$$

and therefore

$$|\Delta R_{m-1}| := \max_{0 \le n \le N} |\Delta R_{m-1}^n| \le |\Delta R_m| + h\,|\Delta W_m| + O\left(h^2\right),$$

$$|\Delta W_{m-1}| := \max_{0 \le n \le N} |\Delta W_{m-1}^n| \le |1 - ah|\,|\Delta W_m| + hC_\alpha \frac{\varepsilon}{\delta} + O(hk) + O\left(h^2\right).$$

Consequently

$$\begin{aligned}
|\Delta R_{m-1}| &\le |\Delta R_m| + h \cdot |\Delta W_m| + O\left(h^2\right) \\
&\le (1+h) \cdot \max\{|\Delta R_m|, |\Delta W_m|\} + O\left(h^2\right),
\end{aligned}$$

and

$$\begin{aligned}
|\Delta W_{m-1}| &\le |1 - ah|\,|\Delta W_m| + hC_\alpha \frac{\varepsilon}{\delta} + O(hk) + O\left(h^2\right) \\
&\le |1 - ah| \cdot \max\{|\Delta R_m|, |\Delta W_m|\} + hC_\alpha \frac{\varepsilon}{\delta} + O(hk) + O\left(h^2\right),
\end{aligned}$$

so that

$$\begin{aligned}
\max\{|\Delta R_{m-1}|, |\Delta W_{m-1}|\} \le (1+h) \cdot \max\{&|\Delta R_m|, |\Delta W_m|\} + \\
&hC_\alpha \frac{\varepsilon}{\delta} + O(hk) + O\left(h^2\right)
\end{aligned}$$

for $m = M, M-1, \ldots, 1$, and for any $0 < h < 1/a$. It is readily verified by induction that

$$\begin{aligned}
\max\{|\Delta R_0|, |\Delta W_0|\} \le (1+h)^M \max\{&|\Delta R_M|, |\Delta W_M|\} + \\
&\sum_{m=0}^{M-1} (1+rh)^m \left(hC_\alpha \frac{\varepsilon}{\delta} + O(hk) + O\left(h^2\right) \right).
\end{aligned}$$

Hence

$$\begin{aligned}
\max\{|\Delta R_0|, |\Delta W_0|\} \le e \cdot \max\{&|\Delta R_M|, |\Delta W_M|\} + \\
&\sum_{m=0}^{M-1} (1+h)^m \left(hC_\alpha \frac{\varepsilon}{\delta} + O(hk) + O\left(h^2\right) \right)
\end{aligned}$$

for all sufficiently small $h > 0$. Since

$$\sum_{m=0}^{M-1} (1+h)^m = \frac{1 - (1+h)^M}{1 - (1+h)} = \frac{(1+h)^M - 1}{h} = \frac{\left(1 + \frac{1}{1/h}\right)^{1/h} - 1}{h} < \frac{e}{h},$$

$$\max\{|\Delta R_0|, |\Delta W_0|\} \le e \cdot \max\{|\Delta R_M|, |\Delta W_M|\} + e\,C_\alpha \frac{\varepsilon}{\delta} + O(k) + O(h),$$

and by lemma 3.2 we obtain the estimate

$$\max\{|\Delta R_0|, |\Delta W_0|\} \leq C\left(\delta + \frac{\varepsilon}{\delta} + k\right) + O(k) + O(h)$$

for some constant $C > 0$. To get convergence, the choice $\delta = O\left(\varepsilon^{1/2}\right)$ shows that $\max\{|\Delta R_0|, |\Delta W_0|\} = O\left(\varepsilon^{1/2} + k + h\right)$, which implies formal convergence as ε, h and $k \to 0$. ☑

4. Data generation for TFIADP

In order to generate the necessary data for modeling the TFIADP, it is necessary to first solve the corresponding TFADP (the direct problem). Since a simple exact solution for the direct problem is not available, we implement an implicit finite difference scheme based on the scheme proposed by Murio [11], and then use the finite difference approximation as a reference solution, the closest we are from the exact solution.

The TFADP to solve is

$$\begin{aligned}
D_t^{(\alpha)} v(x,t) + av_x(x,t) &= v_{xx}(x,t), \quad 0 < x < 1, \ \ 0 < t < \tau, \\
v(0,t) &= v_l(t), \quad 0 < t \leq \tau, \\
v(1,t) &= v_r(t), \quad 0 < t \leq \tau, \\
v(x,0) &= f(x), \quad 0 \leq x \leq 1.
\end{aligned} \tag{26}$$

The description of the scheme is as follows: Let M and N be positive integers and let $\Delta x = h = \frac{1}{M}$ and $\Delta t = k = \frac{\tau}{N}$ be the finite difference grid sizes. For each $m \in \{0, \dots, M\}$, and each $n \in \{0, \dots, N\}$, let v_m^n be the computed approximations of $v(x_m, t_k)$, where $x_m = mh$, and $t_n = nk$ are the grid point in the space interval $[0,1]$ and time interval $[0,\tau]$, respectively. We approximate the partial differential equation $D_t^{(\alpha)} v + av_x = dv_{xx}$ with the consistent finite-difference scheme

$$\sigma_{\alpha,k} \sum_{m=1}^{n} \omega_m^{(\alpha)} \left(v_m^{n-m+1} - v_m^{n-m}\right) + a\frac{v_{m+1}^n - v_{m-1}^n}{2h}$$
$$= d\frac{v_{m-1}^n - 2v_m^n + u_{m+1}^n}{h^2}, \quad (27)$$

obtaining for internal nodes ($m = 1, 2, \dots, M-1$) and $n = 1$,

$$-\left(\frac{1}{h^2} + \frac{c}{2h}\right)v_{m-1}^1 + \left(\sigma_{\alpha,k} + \frac{2}{h^2}\right)v_m^1 - \left(\frac{1}{h^2} - \frac{c}{2h}\right)v_{m+1}^1 = \sigma_{\alpha,k}v_m^0,$$

and for $n = 2, \ldots, N$,

$$-\left(\frac{1}{h^2} + \frac{c}{2h}\right) v_{m-1}^n + \left(\sigma_{\alpha,k} + \frac{2}{h^2}\right) v_m^n - \left(\frac{1}{h^2} - \frac{c}{2h}\right) v_{m+1}^n$$

$$= \sigma_{\alpha,k} v_m^{n-1} - \sigma_{\alpha,k} \sum_{m=2}^n \omega_m^{(\alpha)} \left(v_m^{n-m+1} - v_m^{n-m}\right),$$

with boundary conditions

$$v_0^n = v_l(t_n), \quad v_M^n = v_r(t_n), \quad n = 1, \ldots, N$$

and initial condition

$$v_m^0 = f(x_m), \quad m = 0, \ldots, M,$$

where $\sigma_{\alpha,k}$ and $\omega_m^{(\alpha)}$ are given by (10).

The procedure to generate data for Algorithm 1 consists on using scheme (27) for obtaining approximate solutions of the direct problems

$$
\begin{aligned}
D_t^{(\alpha)} w + aw &= dw_{xx}, \quad 0 < x < 1, \quad t > 0, \\
w(0, t) &= w_0^\varepsilon(t), \quad t > 0, \\
w(1, t) &= w_1^\varepsilon(t), \quad t > 0, \\
w(x, 0) &= f(x), \quad 0 \le x \le 1,
\end{aligned}
\tag{28}
$$

and

$$
\begin{aligned}
D_t^{(\alpha)} z + az &= dz_{xx}, \quad 0 < x < 1, \quad t > 0, \\
z(0, t) &= 0, \ t > 0, \\
z(1, t) &= 0, \ t > 0, \\
z(x, 0) &= f(x), \quad 0 \le x \le 1.
\end{aligned}
\tag{29}
$$

Setting $v(x, t) := w(x, t) - z(x, t)$, data $v(1, t) = w(1, t) - z(1, t) = w_1^\varepsilon(t)$ and $v_x(1, t) = w_x(1, t) - z_x(1, t)$ are used to initialize Algorithm 1. In this way we obtain $v(0, t) = w(0, t) - z(0, t) = w_0^\varepsilon(t)$ and $v_x(0, t) = w_x(0, t) - z_x(0, t)$ as "exact solution" of the inverse problem (18). The derivatives $v_x(0, t_n)$ and $v_x(1, t_n)$ are computed by the forward difference schemes

$$w_x(0, t_n) = \frac{w_1^n - w_0^n}{h} + O(h), \qquad z_x(0, t_n) = \frac{z_1^n - z_0^n}{h} + O(h)$$

and

$$w_x(1, t_n) = \frac{w_M^n - w_{M-1}^n}{h} + O(h), \qquad z_x(1, t_n) = \frac{z_M^n - z_{M-1}^n}{h} + O(h).$$

Perturbed approximations of the data for the TFIADP (18) at $x = 1$ are simulated by adding random errors

$$\rho^\varepsilon(t_n) := \rho(t_n) + \varepsilon_n, \quad \sigma^\varepsilon(t_n) := \sigma(t_n) + \varepsilon_n, \quad n = 1, \dots, N,$$

where the ε_n's are random number uniformly distributed in $[-\varepsilon, \varepsilon]$, and the magnitude ε indicates a noise relative level.

5. Numerical examples

In order to test the stability and accuracy of the algorithm, we consider a selection of average noise perturbations, and space and time discretization parameters, h and k. The solute concentration and flux of solute errors at the boundary $x = 0$ are measured by the root mean square

$$\frac{\left(\dfrac{1}{N+1}\sum_{n=0}^{N}|R_M^n - \xi(t_n)|^2\right)^{1/2}}{\left(\dfrac{1}{N+1}\sum_{n=0}^{N}|\xi(t_n)|^2\right)^{1/2}} \quad \text{and} \quad \frac{\left(\dfrac{1}{N+1}\sum_{n=0}^{N}|W_M^n - \beta(t_n)|^2\right)^{1/2}}{\left(\dfrac{1}{N+1}\sum_{n=0}^{N}|\beta(t_n)|^2\right)^{1/2}},$$

where the "exact" values $u(0, nk)$ and $u_x(0, nk)$ are the computed (approximate) solutions for the solute concentration, and flux of solute of the direct problem, as explained in section 4.

Example 5.1. This experiment consists on the recovery of a unit step boundary distribution of solute concentration at $x = 0$ from interior data measurements at $x = 1$.

We solve the TFADP's (28) and (29) using (27) with boundary conditions

$$w_0(t) := \begin{cases} 1, & 0.2 \le t \le 0.6, \\ 0, & \text{otherwise}, \end{cases}$$

$w_1(t) = 0$, and time fractional orders $\alpha = 0.10, 0.50, 0.90$, grid sizes $h = 0.01, k = 1/128$ and noise level $\varepsilon = 0.05$. The numerical results for mollified solute concentration v and dispersion flux v_x, after applying the mollified space marching algorithm (1) are shown in Figures (1) and (2).

(A) Solute concentration for $\alpha = 0.1$ (B) Dispersion flux for $\alpha = 0.1$
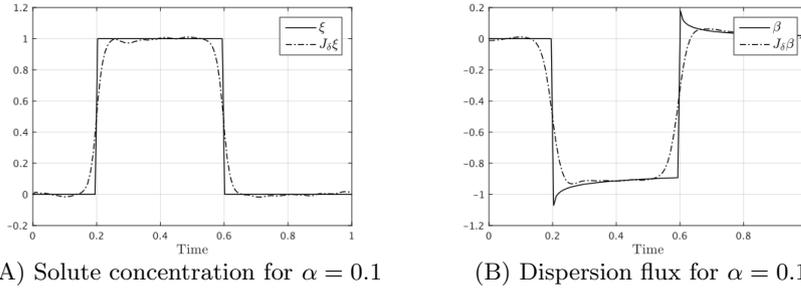
FIGURE 1. Computed and exact solutions with $h = 1/100$, $k = 1/128$ and $\varepsilon = 0.05$.

Numerical results for parameters $h = 1/50, 1/100$ and $k = 1/64, 1/128, 1/256$, and noise levels $\varepsilon = 0.01, 0.05$ are listed in Tables (2) and (3). The relative errors for the reconstructed dispersion fluxes are not shown due to the singularities present in the exact dispersion flux solution functions.

Example 5.2. As a second experiment we solve TFADP (28) with boundary conditions $w_0(t) := 2\sin(4\pi t)$ and $w_1(t) := 1 - e^{-t}$.

Direct problems (28) and (29) are solved using scheme (27) with parameters $h = 1/100$ and $k = 1/128$, time fractional orders $\alpha = 0.10, 0.50, 0.90$ and noise level $\varepsilon = 0.05$. Numerical results are presented in Figures (3) and (4).

| h	k	Solute $\alpha = 0.10$	Solute $\alpha = 0.50$	Solute $\alpha = 0.90$
1/50	1/64	0.162624	0.174689	0.193181
1/50	1/128	0.116263	0.127886	0.166520
1/50	1/256	0.103121	0.113538	0.143003
1/100	1/64	0.195678	0.205159	0.215955
1/100	1/128	0.139927	0.149370	0.164306
1/100	1/256	0.121730	0.129806	0.146498

TABLE 2. Error norms for Problem 1 at $x = 0$ with $\varepsilon = 0.01$.

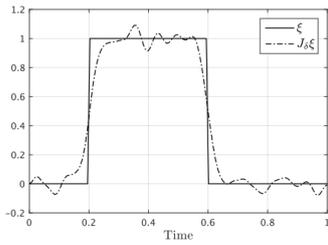| h	k	Solute $\alpha = 0.10$	Solute $\alpha = 0.50$	Solute $\alpha = 0.90$
1/50	1/64	0.177262	0.177804	0.205849
1/50	1/128	0.116877	0.145085	0.202476
1/50	1/256	0.104865	0.122133	0.194356
1/100	1/64	0.195771	0.207485	0.232490
1/100	1/128	0.141560	0.155525	0.193654
1/100	1/256	0.122693	0.134057	0.177372

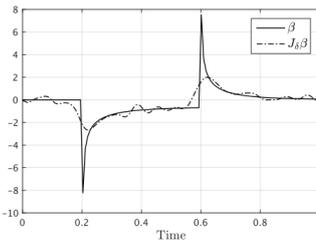TABLE 3. Error norms for Problem 1 at $x = 0$ with $\varepsilon = 0.05$.
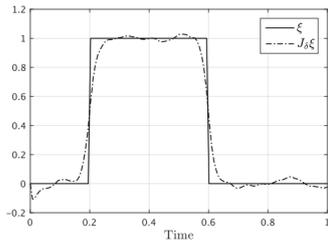
(A) Solute concentration for $\alpha = 0.5$
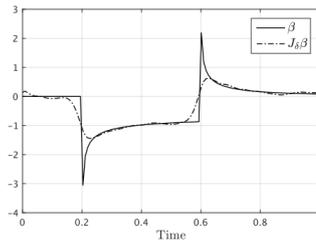
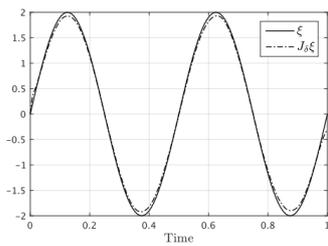(B) Dispersion flux for $\alpha = 0.5$
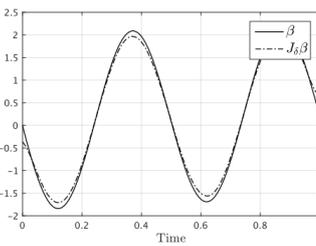
(C) Solute concentration for $\alpha = 0.9$

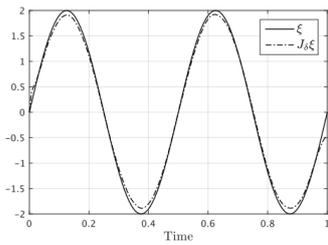(D) Dispersion flux for $\alpha = 0.9$

FIGURE 2. Computed and exact solutions with $h = 1/100$, $k = 1/128$ and $\varepsilon = 0.05$.
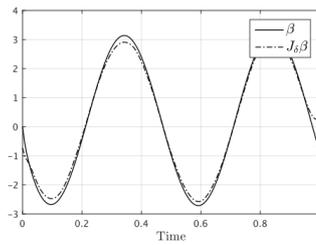
(A) Solute concentration for $\alpha = 0.1$

(B) Dispersion flux for $\alpha = 0.1$

(C) Solute concentration for $\alpha = 0.5$

(D) Dispersion flux for $\alpha = 0.5$

FIGURE 3. Computed and exact solutions with $h = 1/100$, $k = 1/128$ and $\varepsilon = 0.05$.

(A) Solute concentration for $\alpha = 0.9$ (B) Dispersion flux for $\alpha = 0.9$
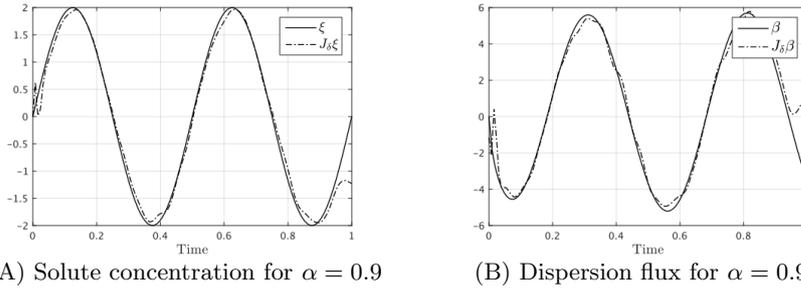
FIGURE 4. Computed and exact solutions with $h = 1/100$, $k = 1/128$ and $\varepsilon = 0.05$.

Further numerical results for parameters $h = 1/50, 1/100$ and $k = 1/64, 1/128$, $1/256$, and noise levels $\varepsilon = 0.01, 0.05$ are listed in Table (4).

h	k	Solute $\alpha = 0.10$	flux $\alpha = 0.10$	Solute $\alpha = 0.50$	Flux $\alpha = 0.50$	Solute $\alpha = 0.90$	Flux $\alpha = 0.90$
$\varepsilon = 0.01$							
1/50	1/64	0.0824357	0.1397440	0.1009910	0.1440130	0.156343	0.213189
1/50	1/128	0.0327805	0.0527263	0.0500833	0.1287310	0.137509	0.223804
1/50	1/256	0.0237803	0.0364998	0.0403763	0.0451279	0.145396	0.258061
1/100	1/64	0.1345390	0.2284960	0.1447270	0.2246910	0.188853	0.276041
1/100	1/128	0.0447909	0.0779111	0.0557262	0.0879756	0.130370	0.216396
1/100	1/256	0.0291530	0.0492424	0.0402326	0.0610357	0.127621	0.234272
$\varepsilon = 0.05$							
1/50	1/64	0.0796441	0.1377250	0.1052100	0.1482640	0.181241	0.234714
1/50	1/128	0.0376843	0.0563460	0.0577398	0.0720823	0.169966	0.294117
1/50	1/256	0.0261905	0.0386800	0.0493100	0.0552515	0.173540	0.349981
1/100	1/64	0.1363810	0.2292630	0.1468220	0.2275990	0.194737	0.278226
1/100	1/128	0.0468243	0.0794672	0.0594679	0.0921621	0.142988	0.228996
1/100	1/256	0.0295951	0.0486042	0.0441289	0.0704283	0.150776	0.266303

TABLE 4. Error norms for Problem 2 at $x = 0$.

6. Final remarks

(1) Problems of the kind TFIADP are relevant in numerical analysis and are potentially useful in different areas of research, including transport problems in groundwater hydrology in the first place.

(2) Discrete mollification with automatic selection of regularization parameters is an appropriate stabilization tool for severely ill-posed TFIADP.

(3) Even knowing that 1-D geometry is adecuate as a first approximation for this inverse problem, an interesting task is to go to dimensions 2 or 3.

(4) Other possible alternatives consists on considering non constant fluid velocity and dispersion coefficients. These changes may lead to nonlinear problems.

Acknowledgments

References

[1] C. D. Acosta, P. A. Amador, and C. E. Mejía, *Stability analysis of a finite difference scheme for a nonlinear time fractional convection diffusion equation*, Analysis, modelling, optimization and numerical techniques (G Olivar and O Vasilieva, eds.), Springer Proceedings in Mathematics and Statistics 121, 2015, pp. 139–150.

[2] C. D. Acosta and C. E. Mejía, *Stabilization of explicit methods for convection diffusion equations by discrete mollification*, Comput. Math. Appl. **55** (2008), 368–380.

[3] D. Benson, S. Wheatcraft, and M. Meerschaert, *Application of a fractional advection-dispersion equation*, Water Resources Research **36** (2000), 1403–1412.

[4] F. Huang and F. Liu, *The time fractional diffusion equation and the advection-dispersion equation*, The ANZIAM Journal **46** (2005), 317–330.

[5] I. Karatay and S. Bayramoglu, *An efficient difference scheme for time fractional advection dispersion equations*, Applied Mathematical Sciences **6** (2012), 4869–4878.

[6] C. Li and F. Zeng, *Numerical methods for fractional calculus*, Chapman and Hall/CRC, 2015.

[7] C. E. Mejía, C. D. Acosta, and K. I. Saleme, *Numerical identification of a nonlinear diffusion coefficient by discrete mollification*, Comput. Math. Appl. **62** (2011), 2187–2199.

[8] C. E. Mejía and D. A. Murio, *Numerical solution of generalized IHCP by discrete mollification*, Comput. Math. Appl. **32** (1996), 33–50.

[9] D. A. Murio, *The mollification method and the numerical solution of ill-posed problems*, John Wiley, 1993.

[10] _____, *On the stable numerical evaluation of Caputo fractional derivatives*, Comput. Math. Applic. **51** (2006), 1539–1550.

[11] _____ , *Implicit finite difference approximation for time fractional diffu-sion equations*, Comput. Math. Appl. **56** (2008), 1138–1145.

[12] _____ , *Time fractional IHCP with Caputo fractional derivatives*, Comput. Math. Appl. **56** (2008), 2371–2381.

[13] D. A. Murio and C. E. Mejía, *Source terms identification for time fractional diffusion equation*, Revista Colombiana de Matemáticas **42** (2008), 25–46.

[14] J. Zhao and S. Liu, *An optimal filtering method for a time-fractional inverse advection-dispersion problem*, J. Inverse Ill-Posed Probl. **24** (2016), 51–58.

[15] G. H. Zheng and T. Wei, *Spectral regularization method for a cauchy problem of the time fractional advection-dispersion equation*, Journal of Computational and Applied Mathematics **233** (2010), 2631–2640.

[16] _____ , *Spectral regularization method for the time fractional inverse advection-dispersion equation*, Mathematics and Computers in Simulation **81** (2010), 37–51.

[17] _____ , *A new regularization method for the time fractional inverse advection-dispersion problem*, SIAM J. Numer. Anal. **49** (2011), 1972–1990.

Escuela de Matemáticas
Universidad Nacional de Colombia - Sede Medellín
Facultad de Ciencias
Calle 59A # 63-20
Medellín, Colombia
e-mail: `cemejia@unal.edu.co`

Instituto de Matemáticas
Universidad de Antioquia
Facultad de Ciencias Exactas y Naturales
calle 70 # 52 - 21
Medellín, Colombia
e-mail: `apiedrahitah@unal.edu.co` - `alejandro.piedrahita@udea.edu.co`